Chapter

Quality Assessment of Installed Rock Bolts

Andrzej Staniek

Abstract

The chapter presents a method for non-destructive identification of discontinuity of a resin layer (grout) surrounding rock bolts. The method uses modal analysis procedures and is based on an impact excitation where a response transducer is positioned at a visible part of a rock bolt. Since the installed rock bolt acts as an oscillator, its modal parameters are changed by different lengths and positions of grouting discontinuity. Thanks to proper extraction of these parameters, with a resonant frequency seen as the most valuable, the intended identification is possible. The measurements and analyses were performed in laboratory conditions and subsequently at experimental and working coal mines where the measurement system was verified. The developed finite element model of the system under test, rock bolt - resin - rock mass, may be used as reference data base for investigated rock bolts. The advantages of the method include plausibility of grouting discontinuity assessment at any time after its installation, a non-destructive character of the method and the fact that it is not necessary to install any additional equipment into a roof section. It enables a localization of a grout discontinuity, whether it is the back part or the front part of a rock bolt.

Keywords: rock, rock bolt, safety, modal analysis, mining

1. Introduction

The role of a rock bolt support system is to secure and reinforce the rock zone in the near field of an underground opening and to fasten it to deeper rock strata [1, 2]. Mostly steel rock bolts are used for that purpose [3, 4]. The rock bolt consists of a steel bar grouted in an oversize hole. A portable installation machine is used to spin the bolt into the hole filled with fast setting epoxy resin cartridges. After hardening of the resin layer a plate and nut are driven up the bolt. Although robust resin cartridges are used, in mining practice the rock bolt may not be fully encapsulated as a consequence of various geotechnical conditions [5–7]: rock divergence, escape of grout into crevices, rock strata movement and improper grouting. The lack of proper grouting may be very hazardous and should be monitored [8]. Current publications in the field of rock bolt diagnosis, indicate that much effort is being taken to estimate the rock bolt integrity and grout quality in the most precise way. Different approaches have been proposed e.g. Granit, Boltometer, RBT and other inventions or methods [9–14]. These methods rely on excitation of a tested rock bolt to vibration along its axis of symmetry and the analysis of output signals. Depending on the proposed method, both acoustic and ultrasonic waves are generated. Correspondingly, different analytical approaches are used as wavelet transform analysis, Fast Fourier Transform (FFT) and neural network algorithms [5, 14–18]. Also smart sensors techniques are introduced for observation of behavior of grouted rock bolts [19], in particular load measurements at the head of them [20], but the problem is not yet fully resolved.

Accordingly, the method for non-destructive identification of grouting discontinuity of rock bolts is proposed to extend the diagnose scope in rock bolting. Thus the diagnosis of void spaces—regions of lack of bonding is seen as crucial here. In the method a transverse excitation is applied which is seen as more adequate for that purpose. At present a diagnose is completed after the analytical phase has been performed in laboratory conditions, so results are not accessible in situ. Its usage is restricted to steel rock bolts up to 2.5 m long, though not only in mining but also in building engineering. It is worth noticing that the same approach to test the integrity of installed rock bolts was described by Godfrey [21]. Though not known to the author at the experimental and analytical stage of the current work, it is very encouraging that similar methodology was presented over forty years ago.

The chapter starts with a theoretical description of the main rules and relationships between investigated modal parameters and measured data. Then the method and structure of a reference base of FE models are presented. Subsequently it is shown how the method was validated in an experimental coal mine. Finally the results of the research realized in working coal mines are discussed.

2. Materials and methods

2.1 Method and critical parameters

Unlike previously mentioned approaches, the proposed method uses modal analysis procedures and excitation forces are generated by an impact hammer. To perform such a quality assessment of grouting rock bolts several conditions must be fulfilled. One of the primary conditions of realization of the method is identification of a modal model of a tested structure. The modal model of a mechanical system basically consists of two matrices [22–25]:

- Fundamental matrix with natural frequencies and damping factors of the modes (eigenvectors),
- Modal matrix which consists of eigenvectors [Φ].

The modal model may be constructed starting from identification of a single modal eigenvector, and a more sophisticated model (not necessarily complete) would be a set of modal eigenvectors coordinates together with their natural frequencies and damping factors. From an individual characteristic of frequency response function $H_{jk}(\omega)$, where *j, k* stand for excitation and response points, evaluation of a natural frequency, a damping factor and a residue for an *r*-mode is possible, Eq. (**1**).

$$H_{jk}(\omega) \rightarrow \omega_r, \eta_r, {}_rA_{jk}; \quad r = 1, m \tag{1}$$

In order to calculate foregoing elements of the modal matrix [Φ], as coordinates of modal vectors ϕ_{jr}, it is necessary to conduct a series of measurements of frequency response functions in different points of a tested mechanical system. The measurement of a frequency response function at excitation point is very important. The coordinates of an r-mode may be calculated knowing a residue ${}_rA_{kk}$ at this point using formula (2):

$$\phi_{kr}{}^2 = {}_rA_{kk} \tag{2}$$

The rest of modal vector coordinates may be calculated using Eq. (3):

$$\phi_{jr} = \frac{{}_rA_{jk}}{\phi_{kr}} \tag{3}$$

where: ϕ_{kr}, ϕ_{jr} - vector coordinates after the process of normalization.

So, for complete presentation of vibration motion of the tested structure with *n* degree of freedom, it is necessary to measure frequency response function at *n* different points of the structure, including a measurement at the excitation point [23, 24, 26, 27]. That is equivalent to the measurement of frequency response functions for a column or vector of a matrix [H]. In practice however, it is quite often appropriate to increase the number of measurement points and perform measurements of additional matrix elements, additional column or row of the matrix, for example hitting the rock bolt in an additional perpendicular direction to an axis of symmetry.

The measurement setup is shown in **Figure 1**. For realization of the method a response transducer was localized at a visible part of the rock bolt, attached using steel ring and stud [26] and a force transducer was localized at an impact hammer head. The direction of excitation was perpendicular to the symmetry axis of the rock bolt as well as is the main axis of the response transducer. After excitation of the rock bolt to transverse vibration, the signals from both the force transducer and the accelerometer (response transducer) were recorded and frequency response function (FRF) was calculated. The excitation was repeated at several points positioned along the outer part of the bar when the accelerometer remained at the same place. The subsequent frequency response functions were stored in universal file format in the computer memory. In the next step data were exported to a workstation where modal parameter extraction methods were realized. Since the installed rock bolt acts as an oscillator, its modal parameters are changed by different lengths and positions of grouting discontinuity. By proper extraction of those parameters, the intended identification was possible.

In this research the natural (resonant) frequency was the main modal parameter taken into account to differentiate foregoing cases of grouting discontinuity. To increase the accuracy of the method frequency response measurements were performed at 5-7 points positioned on the outer part of a rock bolt. It enabled calculating natural frequencies with the use of a larger number of equations and averaging obtained results in the least square sense. Additionally, it was possible to avoid a casual excitation at a nod point of a mode shape [27]. Mode shapes, which is self-understandable, could not be measured on the whole length of a rock bolt (the grouted part of a bar inaccessible). It is only possible in laboratory conditions. **Figures 2** and **3** present the example results of research on known cases of grouting discontinuities in real working conditions where a rock bolt support system was used. The amplitude of FRF function depends on the location of measured points and may differ for each pair of response and reference points, shown on **Figure 3**.

It was also necessary to have a reference point to compare our results with. With this aim the theoretical modal analysis was introduced [23–26] and a base of Finite Element (FE) models were built, encompassing different types of discontinuities (different boundary conditions).

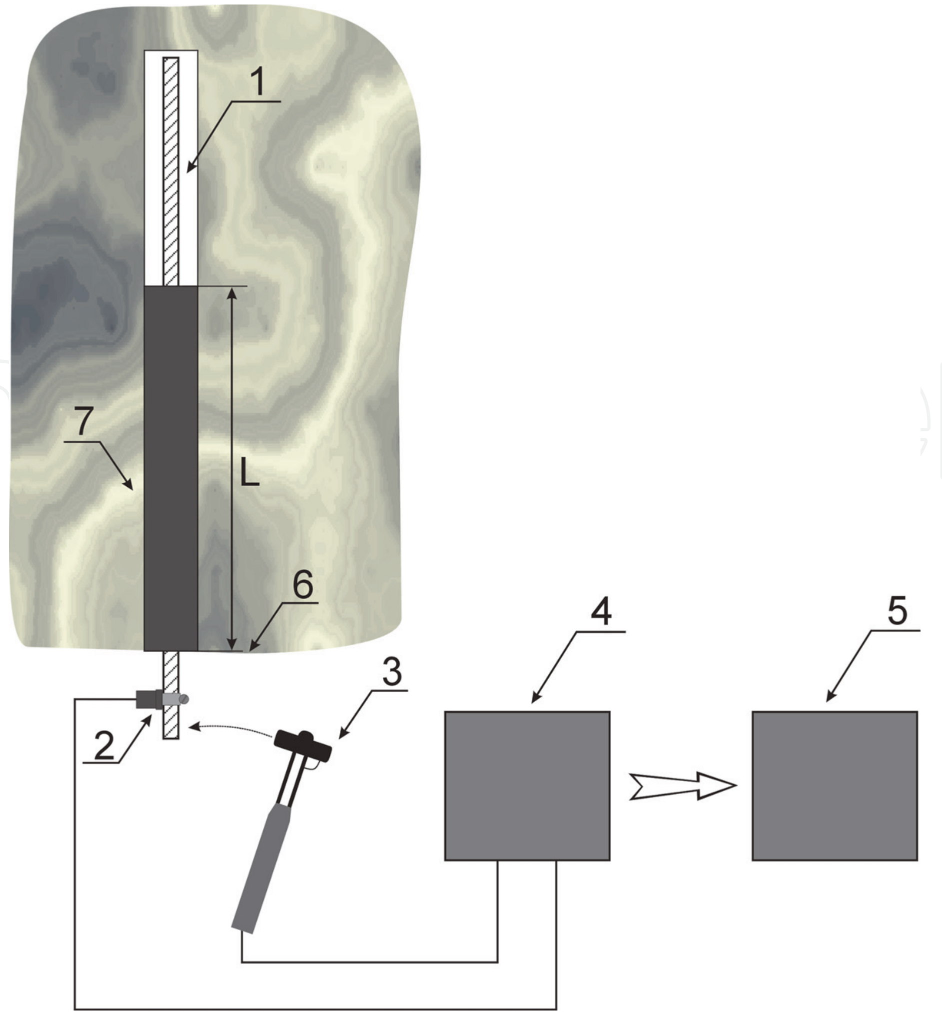

Figure 1.
Measurement setup: (1) rock bolt, typical length 1.5 m-2.5 m; (2) the accelerometer; (3) the impact hammer; (4) portable measurement system; (5) workstation for modal analysis; (6) the surface of the upper roof section; (7) the grout. L is a grouted length.

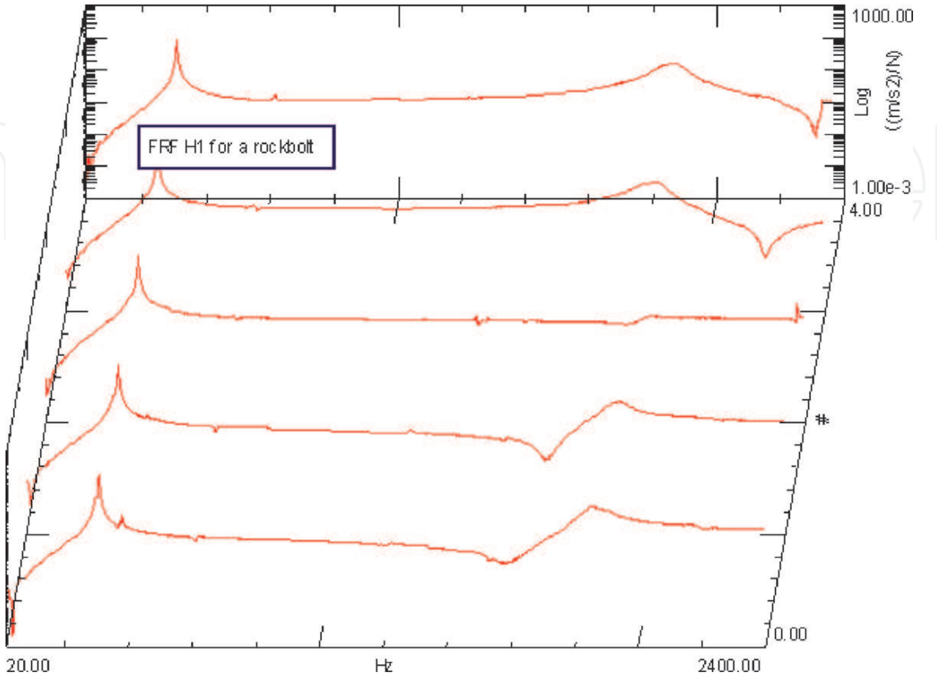

Figure 2.
An example of FRF functions (waterfall curve) for a known case of grouting discontinuities in real working conditions.

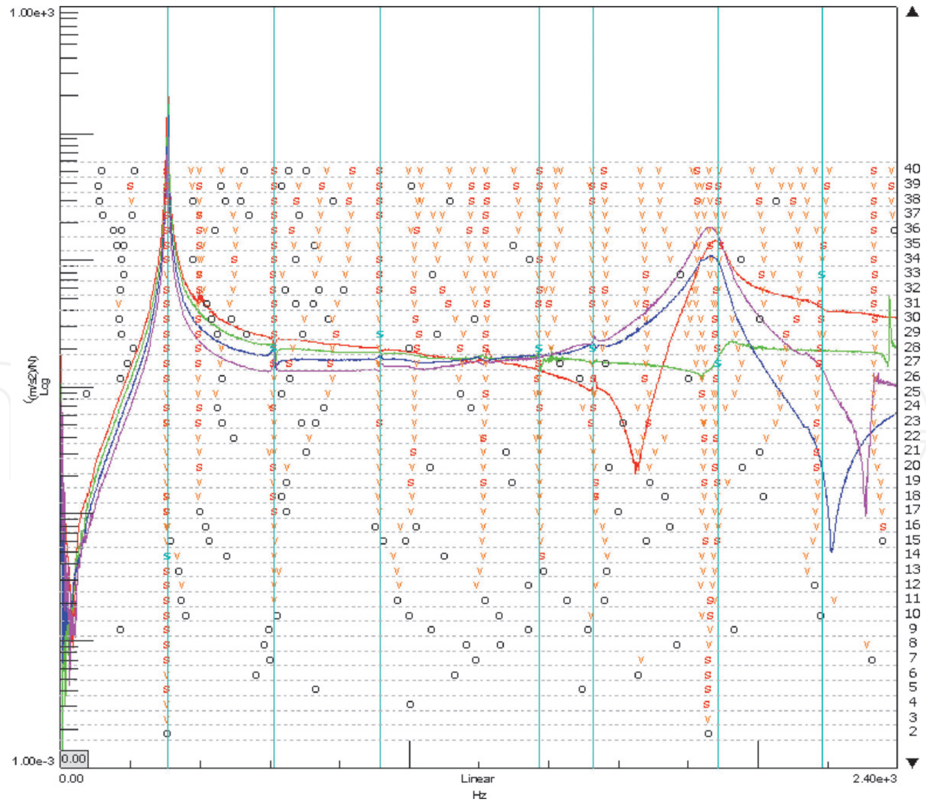

Figure 3.
An example of stabilization diagram for a known case of grouting discontinuities in real working conditions, the FRF curves for all measured points are shown (the order number of the model was set as 40).

2.2 Reference model

The lengths on which a rock bolt (a steel bar) is grouted into a roof section form defined border conditions. Different cases of grouting discontinuity can be modeled in theoretical models. To be used as a reference the theoretical model had to be reconciled to the experimental one taking into account a wide range of cases with controlled, known discontinuities of grouting.

In the presented research ANSYS program was used to build the finite element model of a grouted rock bolt, shown in **Figure 4**. The program enables modeling of finite elements with the help of advanced programming tools, so even very complicated geometry shapes can be developed. In the first phase geometry of the examined structure was involved. Then meshing process was realized and particular

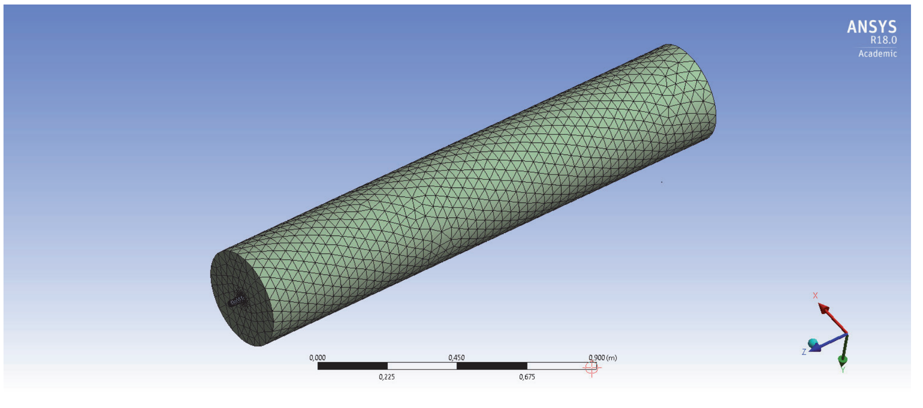

Figure 4.
An example of a finite element model for an analyzed case study.

Property	Component material				
	Steel (bar, nut)	Grout	Cement (optional)	Rock (mudstone)	Rock (sandstone)
Density, kgm^{-3}	7850	1990	2300	2560	2160
Young's Modulus, Pa	2.00E+11	5.110E+09	3.00E+10	6.388E+09	3.722E+09
Poisson's Ratio	0.30	0.10	0.18	0.16	0.09

Table 1.
The properties of components for FE modeling of the investigated rock bolt.

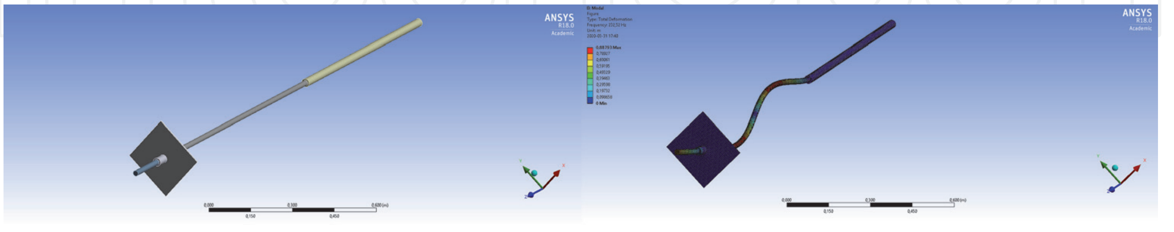

Figure 5.
An example of an analyzed case study and a specific mode of natural frequency 232,5 Hz (the amplitude of the mode is scaled for presentation purposes).

physical properties of materials were introduced including density, Young Modulus, Poisson Ratio etc., shown in **Table 1**. These parameters are crucial since mass and stiffness matrices are built in relation to them. Except steel these parameters were evaluated experimentally. Afterwards adequate physical parameters as well as loads and boundary conditions were attributed to groups of elements. The rock component was ascribed fixed support at the side and back faces and frictional support was attributed to connections between a nut, a plate and roof strata surface. Also, for modeling of torsion force applied to screw the nut and plate to a rock bolt, a bolt pretension feature was utilized (results for different torsion forces were calculated, but that value is controlled by an operator of a bolter and is given). After the process of reconciliation, which comprised all the above mentioned parameters, the validated FE model could be used as a reference base for unknown experimental cases. An example of an analyzed case study and a specific mode of natural frequency is presented in **Figure 5**. The influence of rock strata in which rock bolts are installed was also taken into account but the results obtained both in the experimental and working coal mines (sand stone and mud stone rock strata) showed that the type of rock strata has only a slight impact in comparison with grout discontinuity. As an example, for the particular case, lack of grout at the half length of a rock bolt, the difference ranged from 0.7% to 2.4% for 8 calculated natural frequencies.

As a result of theoretical modal analysis frequency response functions and natural frequencies were calculated (for excitation at the outer part of a rock bolt). Then sets of natural frequencies characteristic of different types of grouting discontinuities were collected and a large data base was set up. **Table 2** presents the sample of data sheets for the carried out calculations and obtained convergence charts of the analyzed cases.

2.3 Utilizing of regression methods

In order to enable fast and effective comparison of theoretical (FE) and experimental models regression methods were reviewed. Cluster analysis seemed to be adequate for that purpose. It is one of the statistical methods to adjust parameters (in the presented research: natural frequencies) measured experimentally with

Lack of grout, cm	f1	f2	f3	f4	f5	f6	f7	f8	f9	F10	F11	F12
5	2325.6	0	0.0	0.0	0.0	0.0	0.0	0.0	0.0	0.0	0.0	0.0
10	917.5		0.0	0.0	0.0	0.0	0.0	0.0	0.0	0.0	0.0	0.0
15	470.3	2487.3	0.0	0.0	0.0	0.0	0.0	0.0	0.0	0.0	0.0	0.0
20	284.1	1686.5	0.0	0.0	0.0	0.0	0.0	0.0	0.0	0.0	0.0	0.0
25	192.6	1175.4	0.0	0.0	0.0	0.0	0.0	0.0	0.0	0.0	0.0	0.0
30	137.1	843.8	2280.2	0.0	0.0	0.0	0.0	0.0	0.0	0.0	0.0	0.0
35	102.7	635.2	1739.9	0.0	0.0	0.0	0.0	0.0	0.0	0.0	0.0	0.0
40	80.0	496.5	1368.4	2552.1	0.0	0.0	0.0	0.0	0.0	0.0	0.0	0.0
. . .	. . .	. . .	. . .	. . .	. . .	. . .	. . .	. . .	. . .	. . .	. . .	. . .
175	4.5	28.2	79.0	154.6	255.3	380.7	530.6	704.8	902.9	1124.5	1369.2	1636.5
180	4.3	26.7	74.7	146.2	241.4	360.0	501.8	666.6	854.1	1063.9	1295.7	1549.0
185	4.0	25.3	70.8	138.6	228.8	341.2	475.7	632.0	809.9	1009.0	1229.0	1470.6
190	3.8	24.0	67.1	131.4	217.0	323.7	451.4	599.8	768.6	957.7	1166.7	1396.2
195	3.6	22.8	63.8	124.8	206.1	307.5	428.8	569.8	730.3	910.1	1108.9	1327.3

Table 2.
The calculated natural frequencies of the finite element models of investigated rock bolts.

calculated data. The concept of cluster analysis, a term introduced in the work of Tryon [28] actually includes several different classification algorithms. For researchers of many disciplines it poses a major problem to organize the observed data in a sensible structure, or data grouping. In other words, cluster analysis is a tool for exploratory data analysis, whose aim is to arrange objects in a group, in such a way that the degree of binding properties of objects belonging to the same group is the largest, and with objects from other groups is as small as possible. Analysis of the cluster can be used to detect data structures without deriving interpretation/ explanation. In short: cluster analysis only detects structure in the data without explaining why it occurs. The general types of methods of cluster analysis are: agglomeration, grouping of objects and characteristics, and k-means clustering. Analysis of the cluster is not a statistical test, but a collection of different algorithms that group objects with specific features. Unlike many other statistical procedures, methods of cluster analysis are used mostly when we do not have any a priori hypotheses, while we are still in the exploratory phase of our research. Therefore, testing the statistical significance in the traditional sense of the term actually is not applicable. Instead measurement discrepancies or the distances between objects are used. The most direct way to calculate the distance between objects in multidimensional space is Euclidean distance calculation. If we have a two-or three-dimensional space, this measure is the actual geometric distance between objects in space. From the point of view of a matching algorithm the actual distances or other derivatives of the distance may be used. The following are the types used.

The first is Euclidean distance. This is a geometric distance in multidimensional space. It should be calculated as follows: distance $(x,y) = \{\Sigma_i (x_i - y_i)^2\}^{½}$.

Euclidean distance (and squared Euclidean distance) are calculated based on the raw data, and not on the basis of the standardized data. This method has some advantages (for example, the distance between any two objects is not affected by adding new objects that can be dispersed). However, the differences of units of dimensions may have a big impact on the way distances are calculated. In general, it is appropriate to standardize them in order to have a comparable data scale.

For squared Euclidean distance the distance is raised to a square, to assign more weight to objects that are more remote. It should be calculated as follows: distance $(x,y) = \{\Sigma_i (x_i - y_i)^2\}^{1/2}$.

Another type of distance is City distance (Manhattan, City block). This distance is simply the sum of the differences measured along the dimensions. In most cases, this distance measure yields similar results to the ordinary Euclidean distance. In the case of this measure, the impact of single large differences (outliers) is suppressed (because they are not raised to the square). City distance is calculated as follows: distance $(x,y) = \Sigma_i |x_i - y_i|$.

We use the distance power when we want to increase or decrease the importance that is assigned to the dimensions for which the relevant properties are quite / completely different. This can be achieved using just the power. It is counted as follows: distance $(x,y) = (\Sigma_i |x_i - y_i|^p)^{1/r}$, where *r* and *p* are parameters defined by the user. The parameter *p* increases / decreases the weight that is assigned to the differences in the individual dimensions, the parameter *r* increases / decreases the weight that is assigned to differences between objects. If *r* and *p* are equal to 2, then the distance is equal to the Euclidean distance.

In the realized research the application was developed to assign experimentally measured natural frequencies to the appropriate corresponding classes of cases of discontinuity calculated on the base of finite element models. The algorithm uses City distance $(x,y) = \Sigma_i |x_i - y_i|$. The match procedure was realized in STATISTICA environment. So, for unknown cases we seek for the lowest value of that distance which represents the best fit to the theoretical model (an estimated grout length and position). **Figure 6** presents the characteristics of the transfer function for the analyzed case, **Table 3** the identified natural frequencies and **Figure 7** the scatter plot of the differences between FE model and data evaluated experimentally.

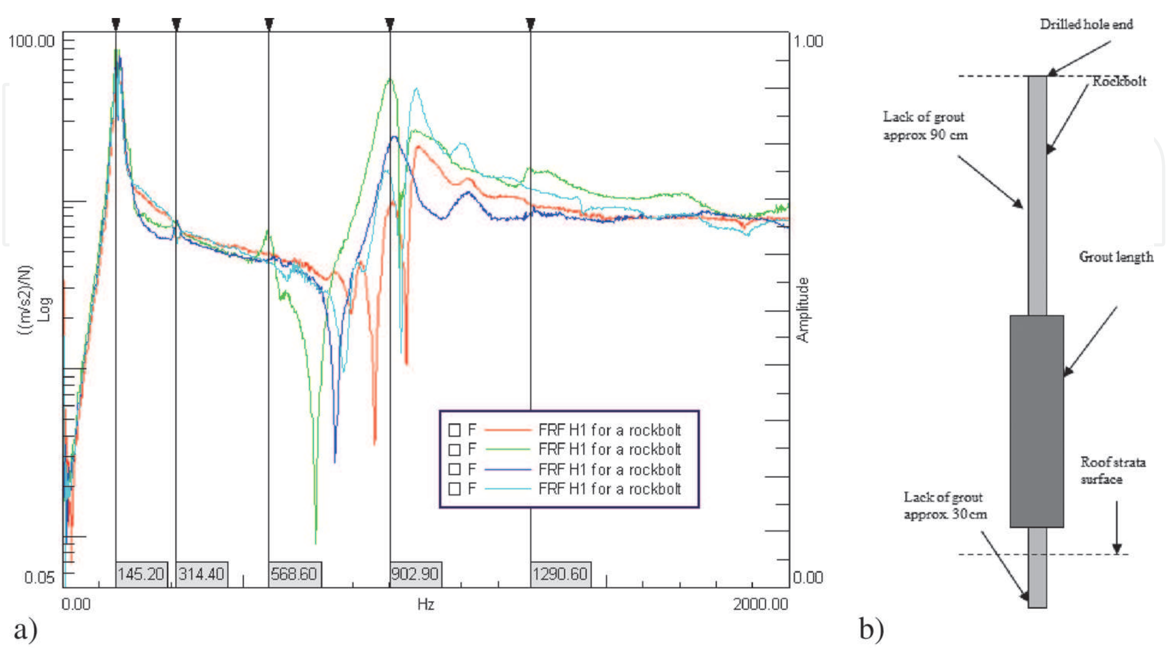

Figure 6.
The characteristics of the transfer function for the analyzed case (a), and the estimated grout length (b), the length of the rock bolt is equal to 1.8 m, the chart axis are: the vertical axis—inertance, in $(m/s^2)/N$, the horizontal axis the frequency, in Hz.

No	Frequency, Hz		Difference, %
	Experiment	FE model	
1	145.2	137.1	−5.6
2*	314.4	291.4	−7.3
3*	568.1	568.6	0.1
4	902.9	843.8	−6.5
5*	1290.6	1387.2	7.5

**The frequency characteristic for the hidden end part of a rock bolt.*

Table 3.
The identified natural frequencies of the investigated rock bolt.

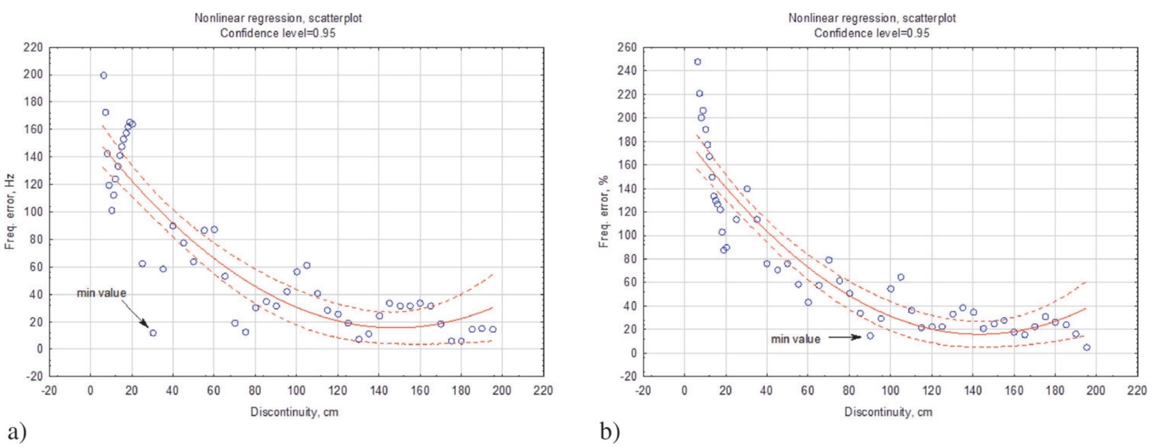

Figure 7.
Scatter plot of the differences between FE model and data evaluated experimentally. The values of the lengths of discontinuity are: (a) 30 cm and (b) 90 cm. These values are specified for the first minimum differences of models and are clearly outside the values of the random scatter.

3. Results and discussion

3.1 Measurements in the experimental coal mine Barbara GIG

The research work on the rock bolts grouted in a controlled way in real coal mine conditions yielded much information about the possibility of identification of grouting discontinuities and the influence of their changes on modal parameters. The measurements were performed in an experimental coal mine Barbara GIG. At the first stage the measurements were performed with previously developed working prototype assembled with National Instruments components, and at the second one, after large modification with the new measurement unit fulfilling ATEX requirements, shown in **Figure 8** (ATEX directives consists of two EU directives describing the minimum safety requirements of the workplace and equipment used in explosive atmosphere. ATEX derives its name from Equipment intended for use in EXplosive ATmospheres).

The total amount of investigated rockbolts in the experimental coal mine was 30. Initially, as it was not known how a supporting plate and a nut may influence the proper identification of grouting discontinuity the diagnose was realized on cases where supporting plate and nut were unscrewed and removed. Later on the experiments were performed with a complete assembly (a plate and a nut fixed), as shown in **Figure 9** and the results were compared (discussed in the second part of this paragraph). The characteristics of transfer functions for the analyzed cases

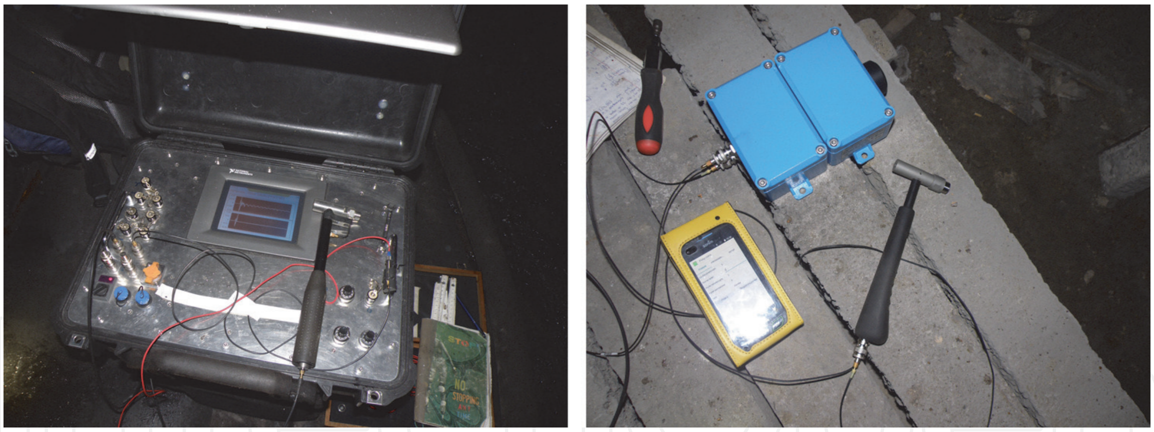

Figure 8.
The portable measurement system for quality control of installed rock bolts, working prototype (left) and final version fulfilling ATEX requirements (right).

were utilized for evaluation of natural frequencies, which were crucial parameters for proper matching with finite element modal models base and diagnosis of related discontinuity length. Basing on in situ measurements and the analysis, we concluded that damping did not convey satisfactory information on the subject and might vary to a certain degree from sample to sample overshadowing its proper usefulness. Since tests in real conditions were performed on a relatively short length of a rock bolt, a mode shape usage was also constrained.

The example results of the undertaken investigations are presented below. The comparison is made for measurements realized with the working prototype and the unit fulfilling ATEX requirements. The analyzed example case corresponds to the discontinuity length shown in **Figure 10**, the lack of grout from the drilled hole end and in the outer part of a rock bolt (supporting plate and nut unscrewed and removed). The differences in upper and lower plots may be attributed to different accelerometer orientation and consequently different impact direction. The identified natural frequencies are shown in **Table 4** and the scatter plots of the differences between FE model and data estimated experimentally for that case are presented in **Figure 11**.

In order to validate this method experiments were continued on the same cases of discontinuity deliberately prepared with the complete assembly of elements, so after screwing plate and nut to the rock bolt. Below the comparison of the measurements performed without the supporting plate and nut, and after screwing

Figure 9.
Impact excitation of installed rock bolts, with the working prototype (left) and the unit fulfilling ATEX requirements (right).

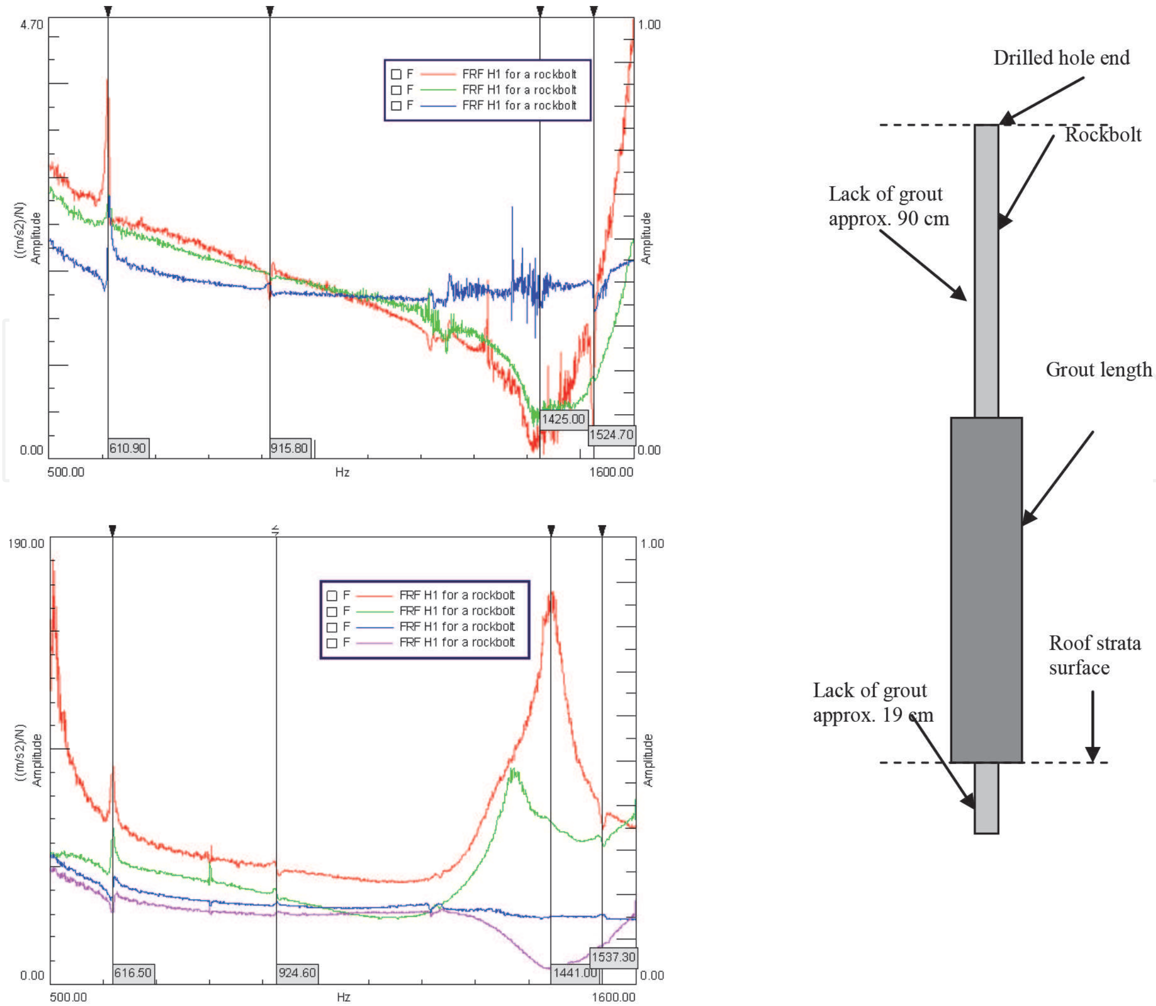

a) b)

Figure 10.
The characteristics of the transfer functions for the analyzed case (measurements realized with the working prototype (a-upper chart) and the unit fulfilling ATEX requirements (a-lower chart)) and the estimated grout length (b), the length of the rock bolt is equal to 2.0 m. The chart axes are: the vertical axis—inertance, in $(m/s^2)/N$, the horizontal axis the frequency, in Hz.

No	Frequency, Hz			Difference (a), %	Difference (b), %
	Experiment (a)	Experiment (b)	FE model		
1	305.7	308.9	311.3	1.8	0.8
2*	610.9	616.5	568.6	−6.9	−7.8
3*	915.8	924.6	934.9	2.1	1.1
4*	1425.0	1441.0	1387.2	−2.7	−3.7
5*	1524.7	1537.3	1387.2	9.0	9.8
6	1707.0	1739.2	1832.9	7.4	5.4

**The frequency characteristic for the hidden end part of a rock bolt.*

Table 4.
The identified natural frequencies of the investigated rock bolt, measurement with the working prototype (a), and the unit fulfilling the ATEX requirements (b).

them to the rock bolt is discussed. A typical torsion force applied in the real working conditions is 250 Nm, so such a value was used in the finite element model (FE). Of course it is not a constraint and other torsion forces may be used according to real situations; a thorough discussion on that topic is accessible in technical literature

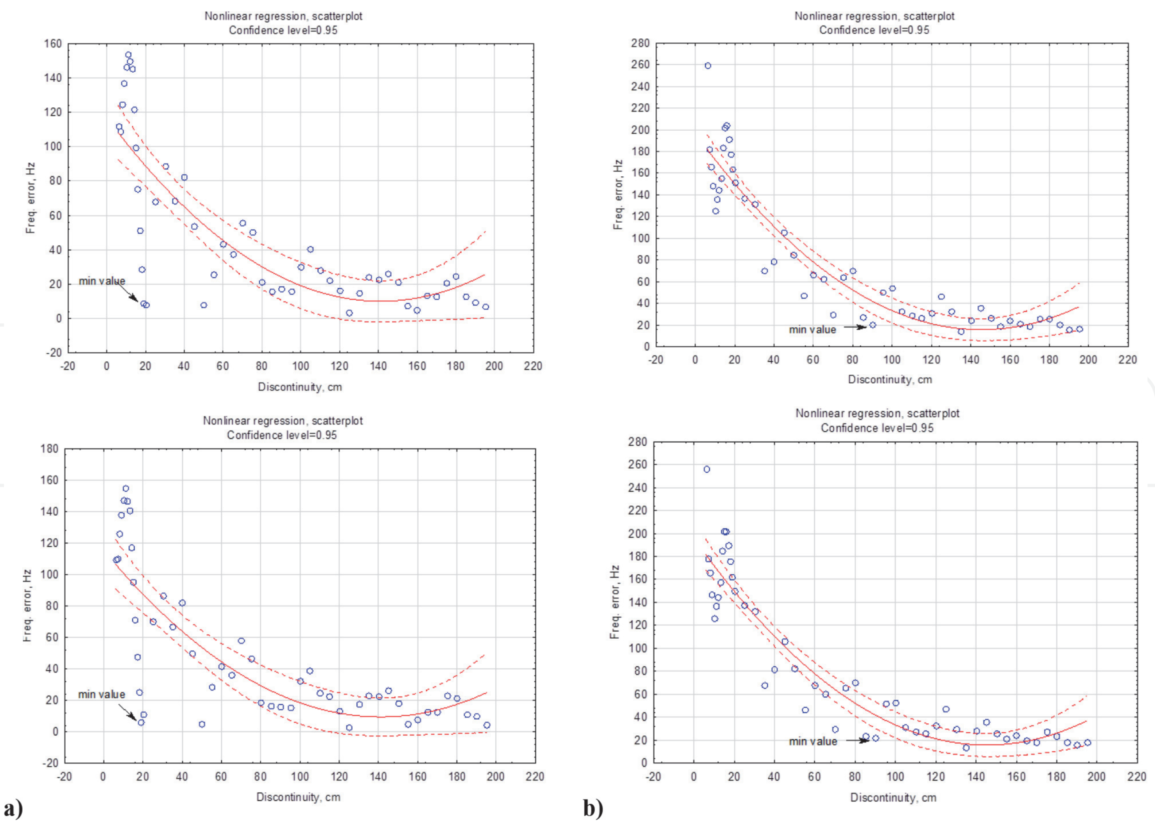

Figure 11.
Scatter plot of the differences between FE model and data evaluated experimentally. The values of the lengths of discontinuity are: (a) 19 cm and (b) 90 cm. These values are specified for the first minimum differences of models and are clearly outside the values of the random scatter. The upper plots are for measurements with the working prototype, the lower ones for measurements with the unit fulfilling the ATEX requirements.

[20, 29]. The example cases (at first without a nut and a plate) are shown in **Figures 12** and **13**. Utilizing the characteristics of the transfer function for the analyzed cases (a), the scatter plots of the differences between FE model and data evaluated experimentally were used and the designated sections of the length of discontinuity were obtained (c). For the rock bolt grouted from a rear, hidden end, shown in **Figure 12**, the discontinuity length is approximately equal to 1.15 m. That value is specified for the first minimum difference of models and is clearly outside the values of the random scatter.

The experimentally identified and numerically calculated (FE model) natural frequencies are presented in **Table 5**.

For the rock bolt grouted from a roof strata surface, shown in **Figure 13**, the discontinuity length is approximately equal to 1.15 m and the length of the outer part is approximately equal to 0.16 m. These values are specified for the first minimum differences of models and are clearly outside the values of the random scatter.

The identified experimentally and calculated numerically (FE model) natural frequencies are presented in **Table 6**.

The results of measurements performed with the supporting plate and nut, after screwing them to the rock bolt are shown in **Figures 14** and **15**. For the rock bolt grouted from a rear, hidden end, shown in **Figure 14**, the discontinuity length is approximately equal to 0.95 m. Though there are two minimum values outside the random scatter, the first one may be chosen as valid, the second may be attributed to aliasing phenomena observed in frequency analysis as well.

The experimentally identified and numerically calculated (FE model) natural frequencies are presented in **Table 7**.

The grout length assessment is quite consistent with that obtained at the first stage, when a plate and a nut were unscrewed.

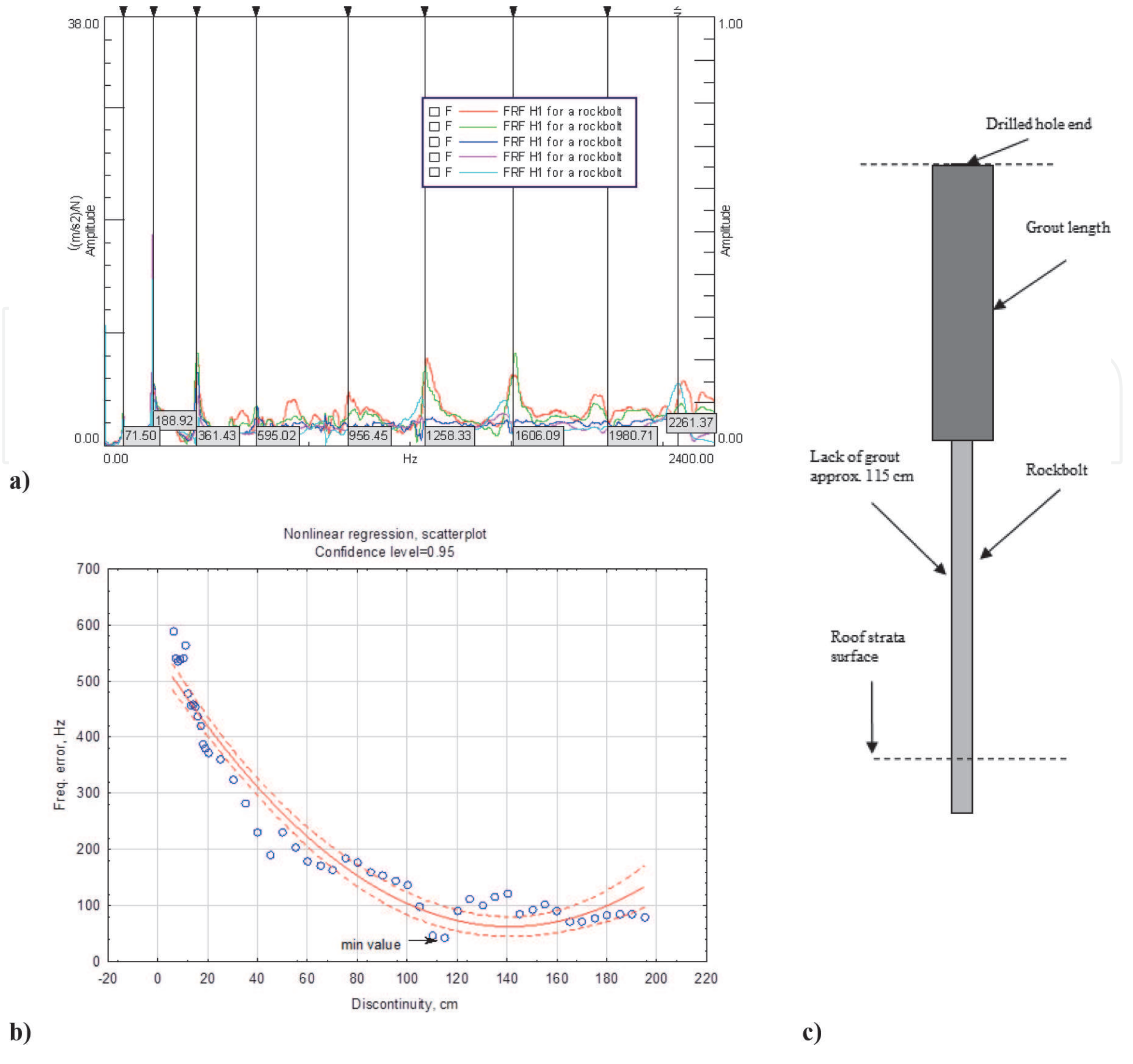

Figure 12.
The results of estimation of the grout length: (a) the characteristics of the transfer function for the analyzed case, the vertical axis of the chart—inertance, in $(m/s^2)/N$, the horizontal axis—frequency, in Hz, (b) the scatter plot of the differences between FE model and data evaluated experimentally, (c) the estimated grout length, the length of the rock bolt is equal to 2.0 m.

No	Frequency, Hz		Difference, %
	Experiment	FE model	
1	71.50	64.78	−9.40
2	188.92	181.09	−4.14
3	361.43	354.0	−2.05
4	595.02	583.34	−1.96
5	956.45	868.02	−9.25
6	1258.33	1206.7	−4.10
7	1606.09	1597.9	−0.51
8	1980.71	2039.3	2.96
9	2261.37	2520.6	11.46

Table 5.
Comparison of identified natural frequencies for a rock bolt grouted from a rear, hidden end, the measurement using working prototype.

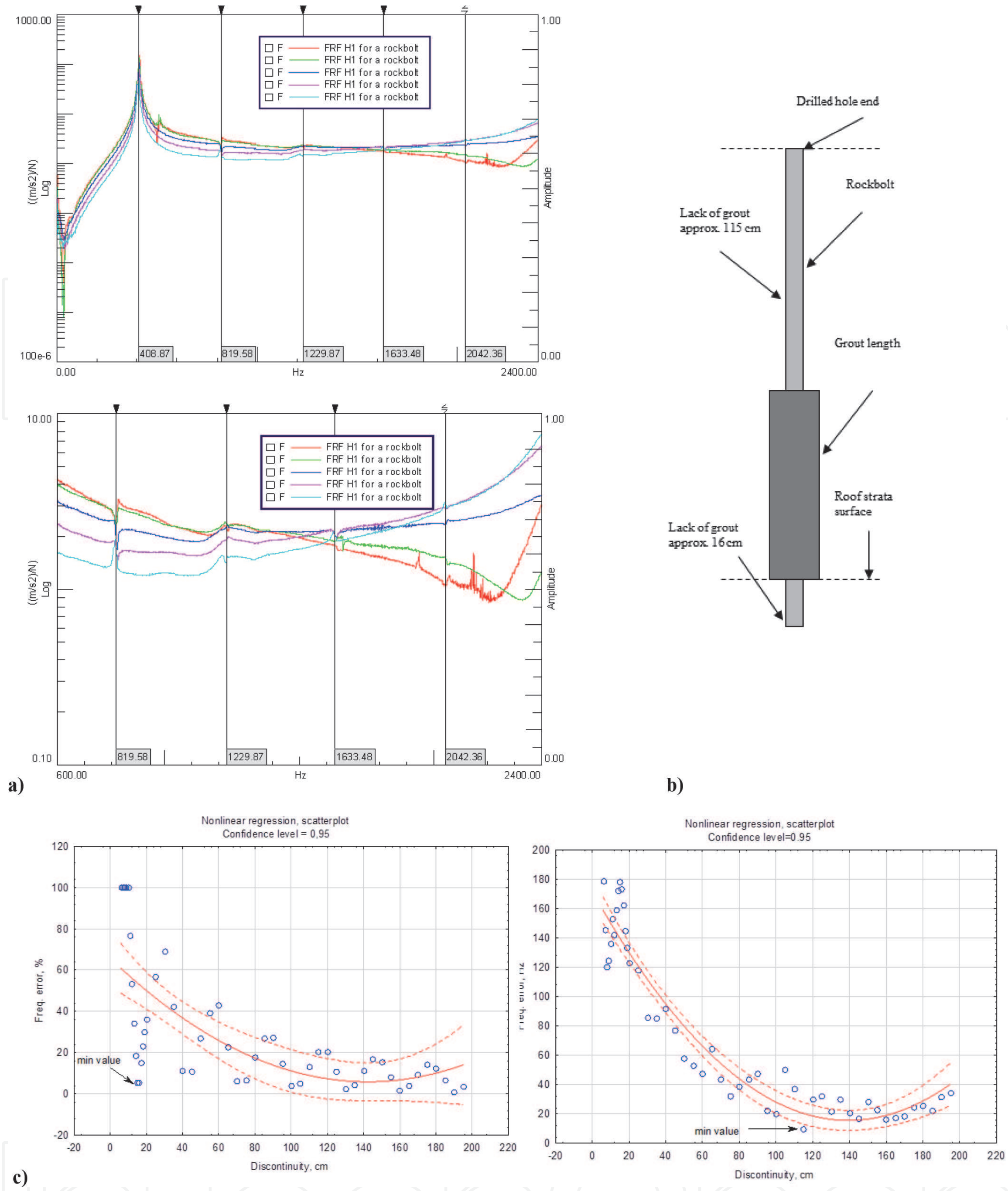

Figure 13.
The results of estimation of the grout length: (a) the characteristics of the transfer function for the analyzed case, the vertical axis of the chart—inertance, in $(m/s^2)/N$, the horizontal axis—frequency, in Hz, (b) the estimated grout length, the length of the rock bolt is equal to 2.0 m, (c) the scatter plot of the differences between FE model and data evaluated experimentally.

For the rock bolt grouted from a roof strata surface, shown in **Figure 15**, the discontinuity length is approximately equal to 1.15 m.

The experimentally identified and numerically calculated (FE model) natural frequencies are presented in **Table 8**.

The grout length assessment is also quite consistent with that obtained at the first stage, when a plate and a nut were unscrewed.

3.2 Measurements in working coal mines

Further experiments were realized in working coal and copper mines and around 50 rock bolts were tested. The aim of one of these experimental studies was connected with rock mass characterization [30] and examination of the strength of

No	Frequency, Hz		Difference, %
	Experiment	FE model	
1	408.873	420.71	−2.81
2*	819.581	868.02	−5.58
3*	1229.866	1206.7	1.92
4*	1633.481	1597.9	2.23
5*	2042.362	2039.3	0.15

**The frequency characteristic for the hidden end part of a rock bolt.*

Table 6.
The identified natural frequencies of the investigated rock bolt grouted from a roof strata surface, the measurement using unit using working prototype.

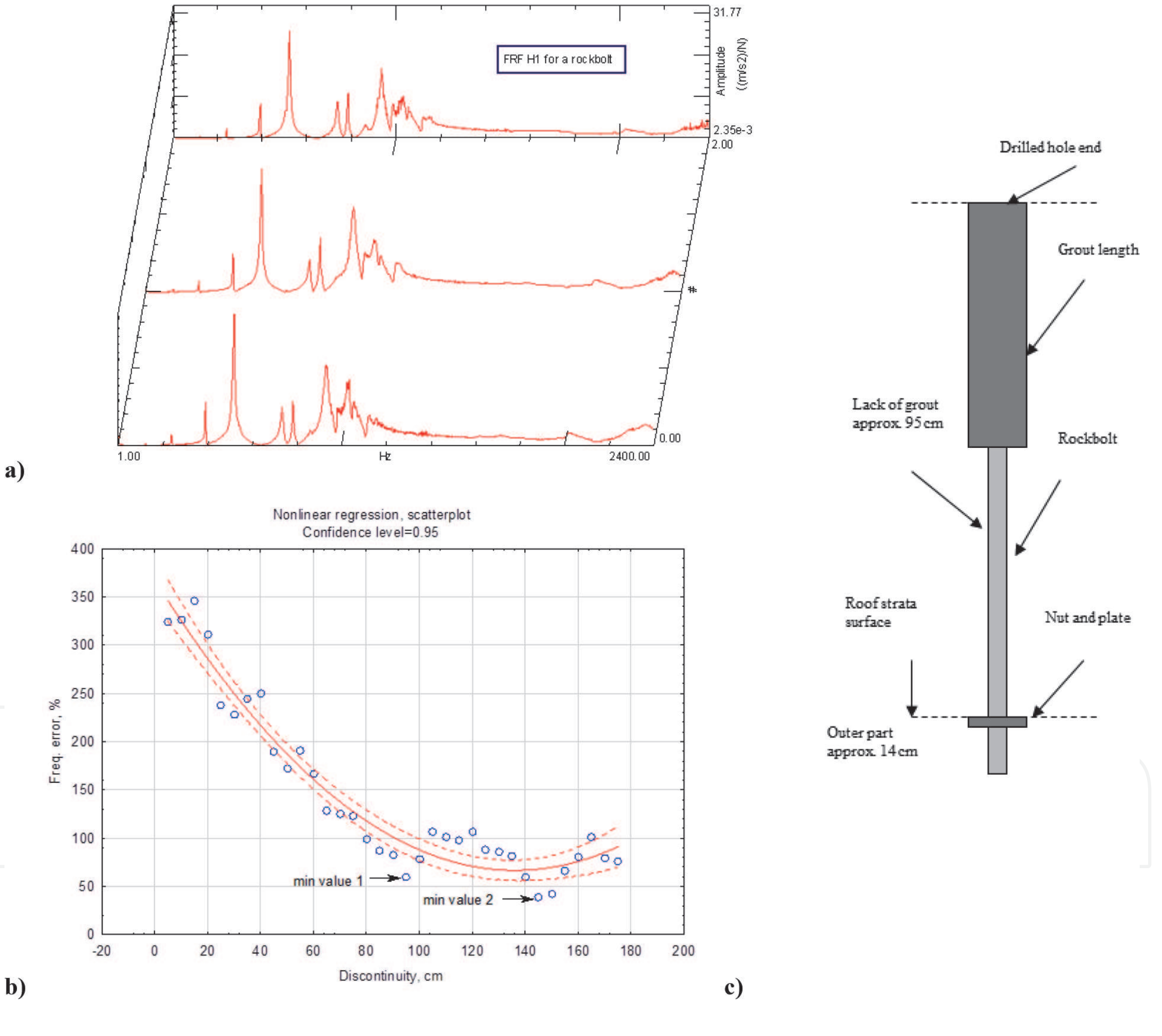

Figure 14.
The results of estimation of the grout length: (a) the characteristics of the transfer function for the analyzed case, the vertical axis of the chart—inertance, in (m/s²)/N, the horizontal axis—frequency, in Hz, (b) the scatter plot of the differences between FE model and data evaluated experimentally, (c) the estimated grout length, the length of the rock bolt is equal to 2.0 m.

rock bolts mounted in the rock strata [3, 4] at different depths. The study took place in a chosen corridor of the working coalmine. The rock bolts were grouted in the roof of the roadway. There were 12 rock bolts mounted in 4 rows and the lengths of the rock bolts were: 2.4 m, 1.85 m, 1.25 m and 0.85 m. Localization of the research and distribution of investigated rock bolts are presented in **Figure 16**. All rock bolts

No	Frequency, Hz			Difference 1, %	Difference 2, %
	Experiment 1	Experiment 2	FE model		
1*	123.2	123.4	101.43	−17.7	−17.8
2*	238.7	238.9	251.25	5.3	5.2
3*	390.6	391.0	346.06	−11.4	−11.5
4	518.7	521.4	528,86	2.0	1.4
5*	783.2	782.9	814.46	4.0	4.0
6*	932.4	935.1	814.46	−12.7	−12.9
7*	1616.5	1609.0	1624.9	0.5	1.0
8*	2017.4	2008.9	1874.9	−7.1	−6.7

**The frequency characteristic for the hidden end part of a rock bolt.*

Table 7.
Comparison of identified natural frequencies for a rock bolt grouted from a rear, hidden end for measurement units—the working prototype based on National Instrument's components and the new one fulfilling the ATEX requirements.

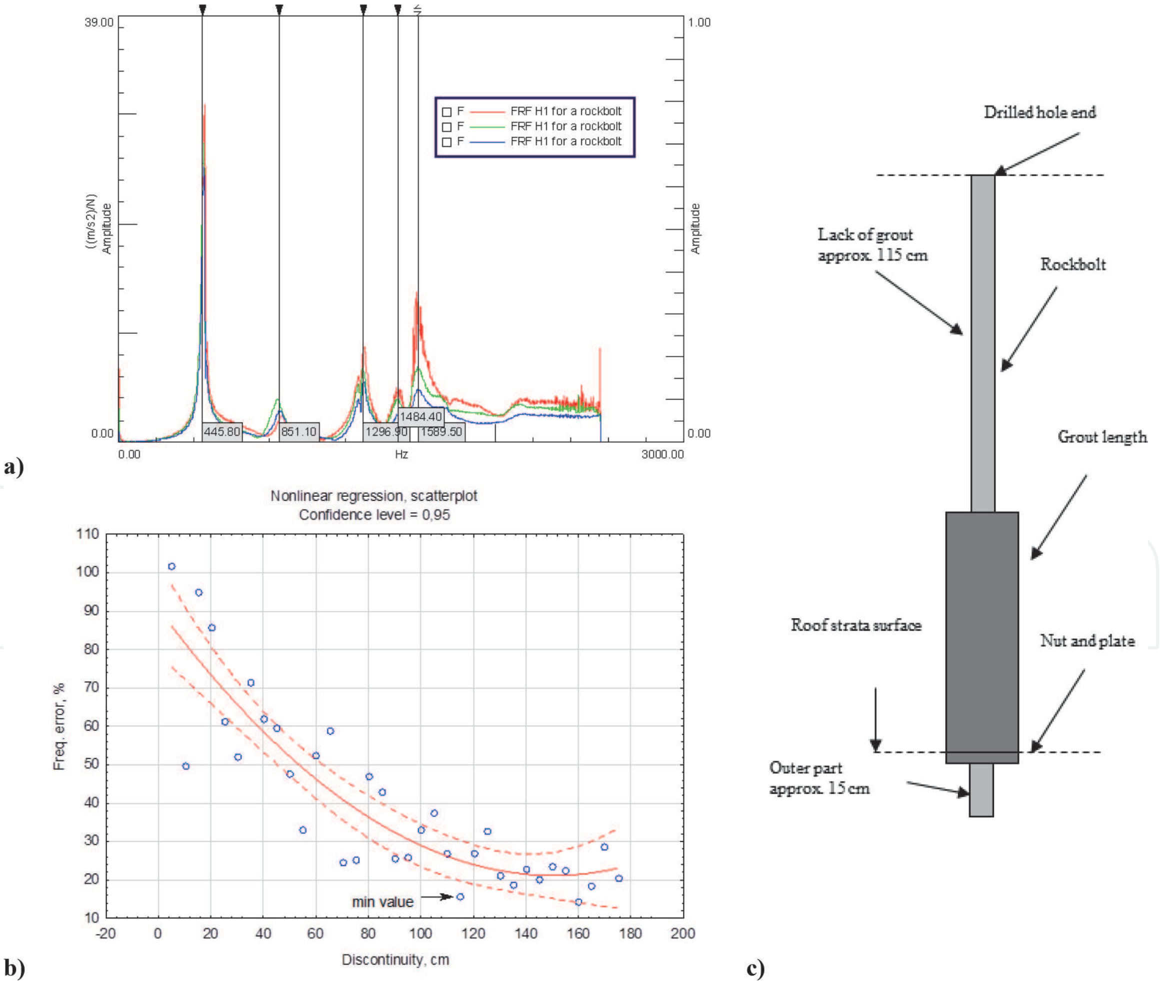

Figure 15.
The results of estimation of the grout length: (a) the characteristics of the transfer function for the analyzed case, the vertical axis of the chart—inertance, in $(m/s^2)/N$, the horizontal axis—frequency, in Hz, (b) the scatter plot of the differences between FE model and data evaluated experimentally, (c) the estimated grout length, the length of the rock bolt is equal to 2.0 m.

No	Frequency, Hz		Difference, %
	Experiment	FE model	
1	445.8	470.3	−5.5
2*	851.1	850.7	0.1
3*	1296.9	1182.2	8.8
4*	1484.4	1564.8	−5.4
5*	1589.5	1667.4	−4.9

**The frequency characteristic for the hidden end part of a rock bolt.*

Table 8.
The identified natural frequencies of the investigated rock bolt, measurement unit—working prototype.

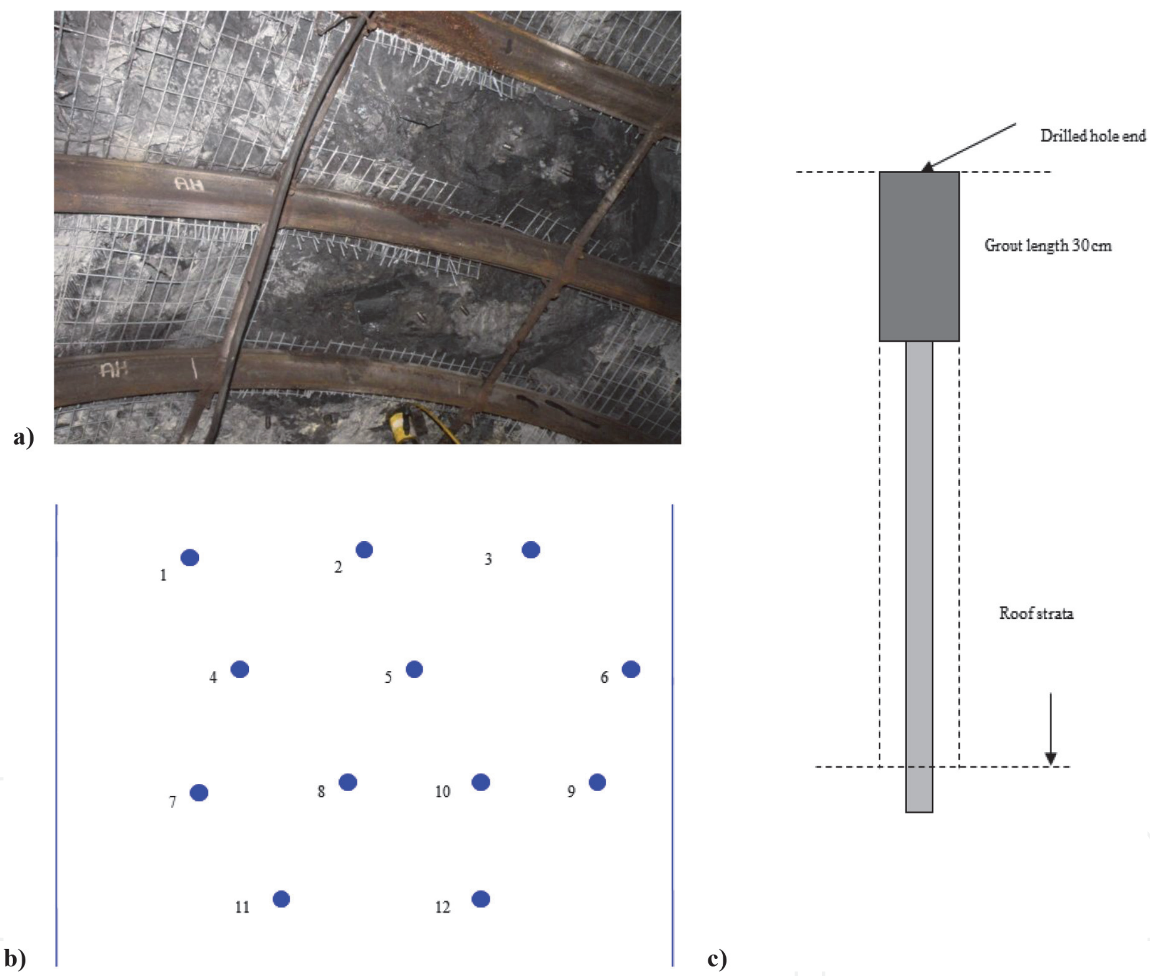

Figure 16.
The exploited seam with investigated rockbolts and hydraulic jack for pull out test (a), distribution of measured rock bolts no 1–12 (b) and the example geometry of the identified discontinuity case (c). The lengths of rock bolts: no 1, 2, 3—2.4 m, no 4, 5, 6—1.85 m, no 7, 8, 9—1.25 m, no 10, 11, 12—0.85 m.

were grouted using the resin material type Lokset. The grout length was 30 cm from the bottom of the hole.

Then a pull out test was conducted by technical staff, who made a thorough analysis of obtained characteristics of pulling (put forward) of the rock bolts taking into account not only pulling of the rock bolt from the grout but also extending of the rock bolt as a result of applied force.

The quality assessment of grouting of rock bolts was performed as complementary to these tests. Although localization and length of the grout were known, the research was undertaken assuming that the result of the grouting process does not necessarily coincide with the intended one. Following are the results of the identification studies of quality assessment of grouted rock bolts. The reference models (FE models), with a specific location of grout, corresponding to experimental cases were matched. The research was conducted for 7 cases and for 4 cases studies were performed before and after pull out tests. For the shortest rock bolts, length 85 cm, lack of sufficient grout strength was also observed (rocks were too weak at that lengths).

The examples of the analysis results in ANSYS environment are shown in **Figures 17** and **18** (visible parts are: a rock bolt and a resin layer). Correct matching cases with calculated mismatch errors are shown in **Tables 9–11**. The diagnosed grout lengths were localized at the end, bottom part of the rock bolts and were very close to the intended grout length of 30 cm. In order to check the accuracy of the assessment the FE calculations were performed also for smaller and larger grout lengths. For example, for the rock bolt with a length of 1.25 m, the smallest difference was obtained for the grout length 31 cm, and by increasing the length of the modeled grout by 1 cm the error changed from positive to negative values, which meant that the correct value was somewhere between 31 cm and 32 cm.

An important observation made during the tests was a slight but distinct increase of identified natural frequencies after pull out tests, which proves the

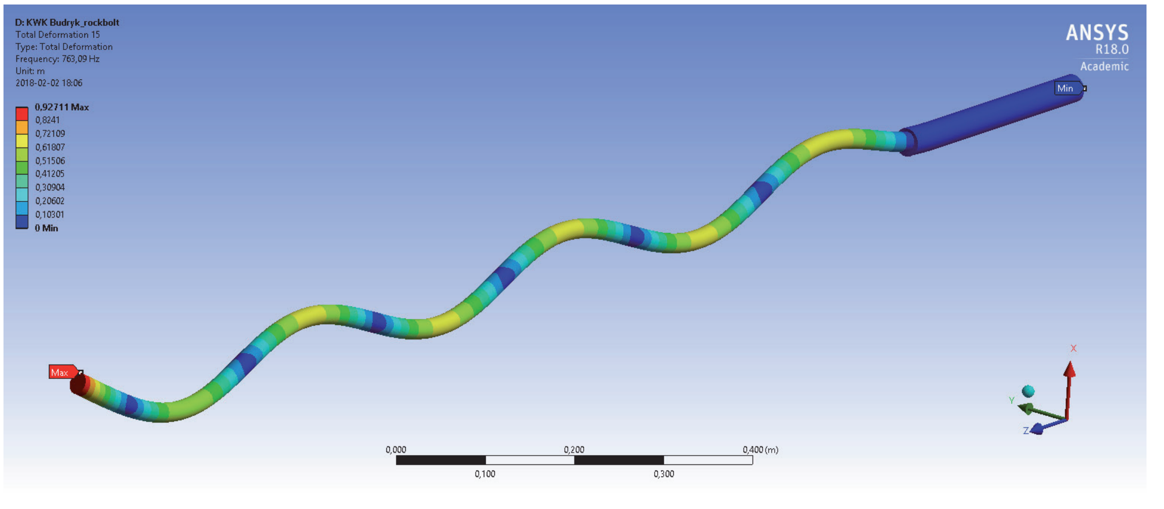

Figure 17.
The example of analysis results in ANSYS environment for a rock bolt length of 1.85 m.

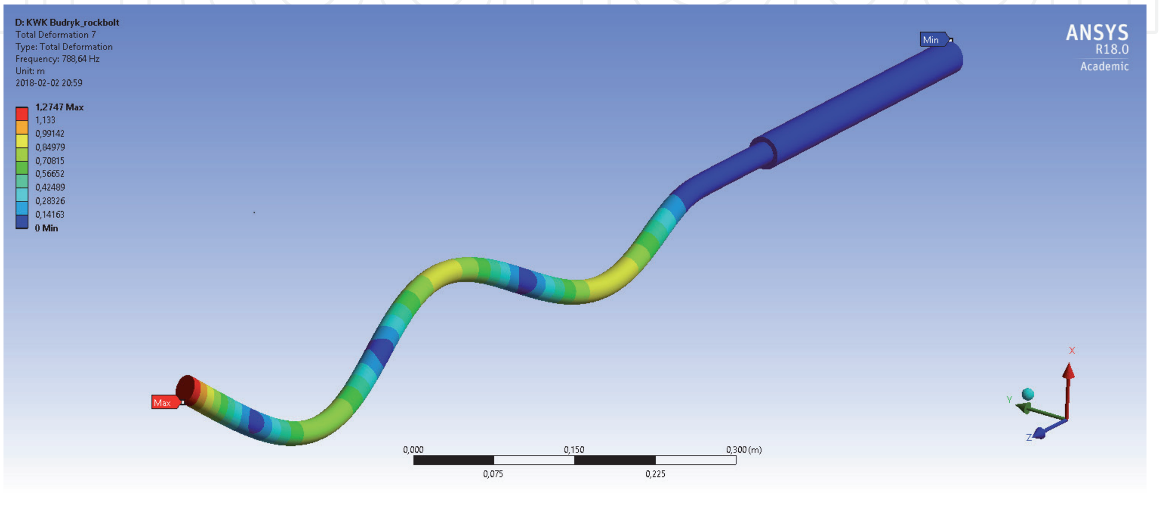

Figure 18.
The example of analysis results in ANSYS environment for a rock bolt length of 1.25 m.

	No 1 before pull out test				No 1 after pull out test		
No	**Frequency. Hz**		**Diff. %**	**No**	**Frequency. Hz**		**Diff. %**
	Experiment	**FE**			**Experiment**	**FE**	
1	204.4	198.0	3.2	1	208.4	198.0	5.2
2	303.9	295.4	2.9	2	308.3	295.4	4.4
3	424.1	411.8	3.0	3	430.3	411.8	4.5
4	565.3	547.1	3.3	4	565.8	547.1	3.4
5	717.8	701.1	2.4	5	741.1	701.1	5.7
6	892.3	873.5	2.2	6	910.2	873.5	4.2
7	1091.1	1064.0	2.5	7	1091.4	1064.0	2.6
8	1307.5	1272.4	2.8	8	1355.9	1272.4	6.6
9	1540.7	1498.2	2.8	9	1589.2	1498.2	6.1
	Average difference. %		2.8		Average difference. %		4.9

Table 9.
Rock bolt length 2.4 m, grout length 0.3 m from the bottom of the hole, case no 1.

	No 5 before pull out test				No 5 after pull out test		
No	**Frequency. Hz**		**Diff. %**	**No**	**Frequency. Hz**		**Diff. %**
	Experiment	**FE**			**Experiment**	**FE**	
1	104.5	111.1	−5.9	1	88.7	111.1	−20.1
2	207.6	217.3	−4.4	2	211.7	217.3	−2.6
3	349.1	358.3	−2.6	3	347.4	358.3	−3.0
4	513.4	533.7	−3.8	4	516.6	533.7	−3.2
5	714.5	743.0	−3.8	5	733.2	743.0	−1.3
6	948.1	985.4	−3.8	6	960.4	985.4	−2.5
7	1206.1	1260.2	−4.3	7	1231.9	1260.2	−2.2
8	1495.4	1566.5	−4.5	8	1581.3	1566.5	0.9
9	1819.8	1902.8	−4.4	9	—	—	—
	Average difference. %		−4.3		Average difference. %		−7.5

Table 10.
Rock bolt length 1.85 m, grout length 0.3 m from the bottom of the hole, case no 5.

impact of the test on mechanical parameters of the test structure and shows a stress hysteresis. Because of the elongation, that is, a slight increase of the length of the rock bolt, this change should go in the opposite direction, namely a decrease of the natural frequencies. In analyzed cases it appears that the first factor is dominant—stress hysteresis. During a normal quality assessment of grouted rock bolts this effect will not take place. It should also be noted that in investigated cases not all natural frequencies were identified, however, their number was sufficient to match the experimental and theoretical (FE) models. The results were quite satisfactory and proved the usefulness of the method.

Based on obtained knowledge and experience research was continued for quality assessment of rock bolt support system realized as a project of above 2 km length corridor drilled for excavation purposes to enable access to large coal deposits. The

No 8 after pull out test				No 8 after pull out test			
No	Frequency. Hz		Diff. %	No	Frequency. Hz		Diff. %
	Experiment	FE			Experiment	FE	
1	—	—	—	1	103.9	102.8	1.1
2	292.4	286.7	2.0	2	295.2	286.7	3.0
3	568.0	559.0	1.6	3	571.0	559.0	2.1
4	932.8	918.0	1.6	4	927.8	918.0	1.1
5	1382.2	1360.3	1.6	5	1376.3	1360.3	1.2
6	1945.7	1880.8	3.4	6	1900.7	1880.8	1.1
Average difference. %			2.2	Average difference. %			1.7

Table 11.
Rock bolt length 1.25 m, grout length 0.3 m from the bottom of the hole, case no 8.

No	Frequency, Hz		Difference, %
	Experiment	FE model	
1	363.8	362.0	−0.5
2	676.3	689.2	1.9
3	1023.0	1061.8	3.8
4	1296.9	1336.3	3.0
5	1468.3	1336.3	−9.0
6	1778.7	1785.2	0.4
7	2135.0	2398.9	12.4

Table 12.
The identified natural frequencies of the investigated rock bolt.

research was performed in several sessions and it seems to be relevant to perform such a control on a periodic basis.

The diagnosed natural frequencies with calculated mismatch errors for the example case are presented in **Table 12**.

The FRF functions (waterfall curve) for an investigated rock bolt, a placement of the response transducer, and the identified discontinuity length are presented in **Figure 19**. The discontinuity length is about 80 cm from the outer part. What was observed in that particular session that in the adjacent area several similar cases of discontinuity were diagnosed.

While explaining possible reasons of improper grouting it is worth considering the technology of installation of rock bolts. There are mainly three phases of fixing the rock bolt into rock strata: a placement of grout cartridges into a drilled hole using a rockbolt (a rock bolt is inserted up to it half length), turning phase with continued insertion of a rock bolt up to the end of the hole (depending on the environmental conditions a time period is about 10 s), spinning phase (about 4-5 s) and hold phase (about 15 s). It is very crucial to control these phases especially the turning and spinning ones. Otherwise lack of grouting connection may occur. Too fast insertion of a rock bolt may lead to leakage of grout from the hole and lack of grout in the back part. Too long spinning phase may cause damage of contact between a rock bolt and grout in the inner part (close to the end of the hole). It is

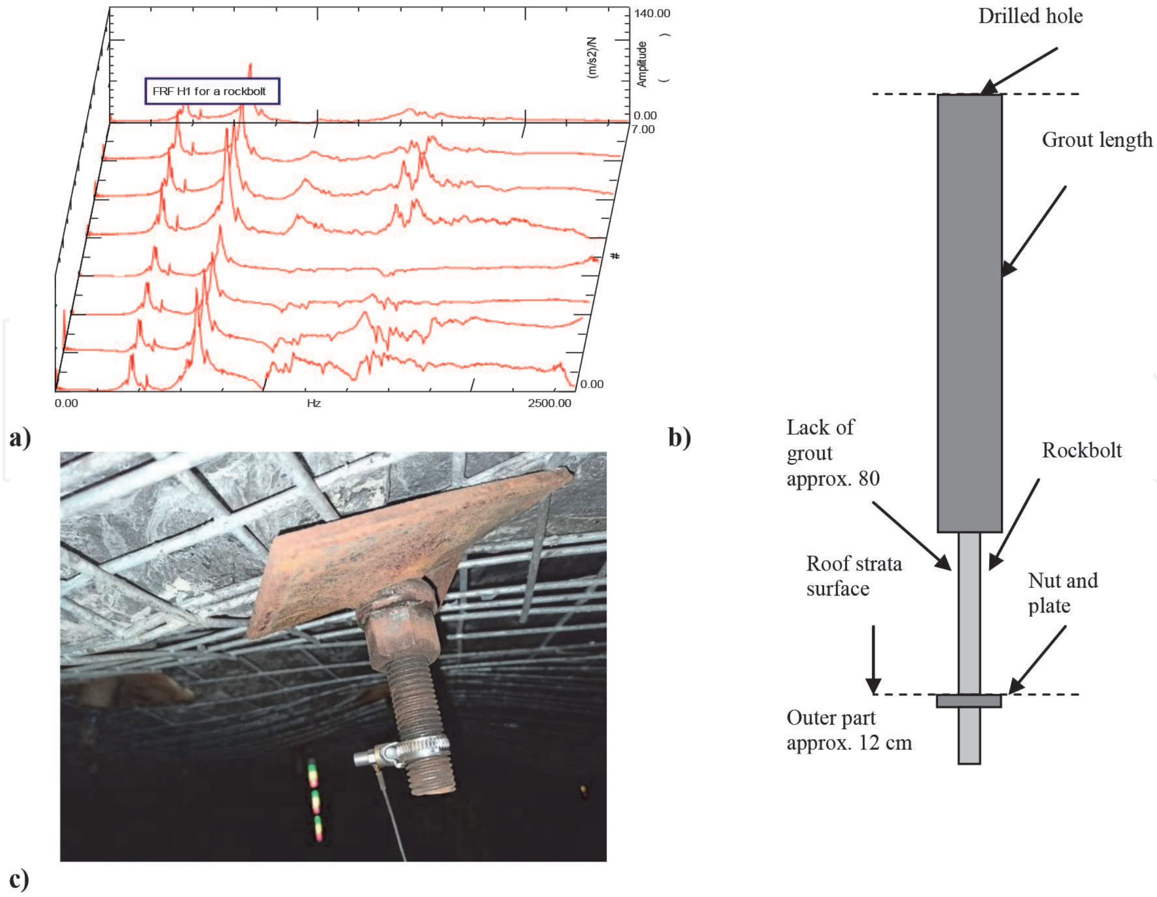

Figure 19.
The results of rock bolt quality assessment, FRF functions (waterfall curve) for an investigated rock bolt (a), the identified discontinuity case (b), a placement of the response transducer (c), the length of the rock bolt is equal to 2.5 m.

because the hardening time in that part is shorter than that in the outer part (specific preparation of grout cartridges). Too slow insertion may result in not full mixing of grout, especially at the end of a rock bolt (one of the consequences might be a rock bolt sticking out more than it is supposed to). If there are crevices in rock strata some amount of grout may leak into that area with the result of local discontinuity of grout layer. Another case might be a larger diameter of the hole then projected, mainly in the outer part of a hole (quite often when rock strata is hard). Then the amount of grout inserted is not enough for proper connection of a rock bolt to rock strata and it also may lead to lack of grout in the outer part of the hole. Inspection of camera records of holes in the investigated area revealed that it could be the reason for not proper grouting for the case shown in **Figure 19**.

4. Conclusions

The increasing interest in the use of rock bolt support systems has its economic background. This system of prevention is less time and material consuming as well as technically more feasible. In strong rocks the use of rock bolt systems is prevailing. In Polish coal mines where rock strata are weaker, the interest in the usage of rock bolt support system is much lower but recently marked changes may be observed in this area. At the same time there is no satisfactory non-destructive method for testing rock bolt installation [6]. It was the reason for undertaking the research on the method for identification of grouting discontinuity for rock bolts. The invented method uses modal analysis procedures and is based on an impact excitation and reconciliation of experimental and theoretical modal models.

In laboratory conditions a cause-effect relation was found between excitation of a rock bolt to transverse vibration and response characteristic of the examined structure. To enable in situ measurement a portable measurement system was invented and constructed. The LabVIEW environment was used as a programming tool. Simultaneously, import of recorded data and derivation of modal parameters were performed utilizing modal analysis software LMS TestLab.

Dynamic parameters of a tested structure (installed rock bolt) are determined by its border conditions, which are directly connected with a grouting discontinuity length. That fact enabled us to diagnose the discontinuity length.

It was necessary to build a theoretical modal model of an installed rock bolt where different cases of grouting discontinuity were encountered. The results of theoretical modal analysis performed on validated FE model constituted a reference base for unknown cases (correlation and comparison techniques were used to validate the model). The reference to the base of validated theoretical models was found reasonable (the discontinuities of verification tests were determined a priori). The reference base may be used for different types of rocks.

Based on the prototype construction the final version fulfilling ATEX requirements was constructed.

The transverse excitation was found as more adequate to identify the discontinuity length of the resin layer of the installed rock bolts.

A mass of a response transducer has influence on the results [26], hence it is desired to minimize it.

The measurement system was verified in real coal mine conditions.

On the basis of the carried out research and calculations of finite element models of the system under test, rock bolt - resin - rock mass, it can be concluded that the developed method and analytical application actually classifies the measured natural frequencies group and enables to identify cases of discontinuity (regions of lack of bonding, which is seen as crucial here).

At present a diagnosis is completed after analytical phase performed in laboratory conditions, so results are not accessible in situ. Its usage is restricted to steel rock bolts up to 2.5 m long (longer rock bolts were not investigated), though not only in mining but also in building engineering.

Acknowledgements

The realized research was financed by Polish Ministry of Science and High Education, project no 11060317.

Author details

Andrzej Staniek
Central Mining Institute, Katowice, Poland

*Address all correspondence to: astaniek@gig.eu

References

[1] Li Charlie C. Principles of rock bolting in high stress rock masses, Mining & Environment, **Vol. 2/1**: 133-143. Central Mining Institute, Poland (2010).

[2] Li Charlie C. Principles of rock bolting design. Journal of Rock Mechanics and Geotechnical Engineering, **Vol. 9**, Issue 3: 396-414, 2017. https://doi.org/10.1016/j.jrmge.2017.04.002.

[3] Tadollini S.C. Current roof bolting applications, technologies and theories in US mines", Mining & Environment, Vol. 2/1:305-314. Central Mining Institute, Poland (2010).

[4] Ulusay R., Hudson J.A. The Complete ISRM Suggested methods for rock characterization, Testing and Monitoring: 1974-2006. Ankara, Turkey (2007).

[5] Beard M.D., Lowe M.J.S. Non-destructive testing of rock bolts using ultrasonic waves. International Journal of Rock Mechanics and Mining Sciences 40: 527-536 (2003).

[6] Hebblewhite B., Fabjanczyk M., Gray P. Investigations into premature rock bolt failures in the Australian coal mining industry. Underground Coal Operators' Conference, 167 (2003).

[7] Kidybiński A, Nierobisz A, Masny W Maintenance of an opening affected by tremor enforced within nether roof strata. Proceedings of the Rockbursts 2005 Conference: 41-52. Central Mining Institute, Poland (2005).

[8] Hartman W., Esterhuizen H. A geotechnical risk assessment tool for underground mine drives – The Fourth Australasian Ground Control in Mining Conference, 48 (2018).

[9] Bačić M., Gavin K., Kovačević S. Trends in non-destructive testing of rock bolts. Journal of the Croatian Association of Civil Engineers GRAĐEVINAR, 71(2019) 10: 823-831, https://doi.org/10.14256/JCE.2727.20.

[10] Bergman SGA, Krauland N, Martna J, Paganus T. Non-Destructive Field Test of Cement-Grouted Bolts With the Boltometer, 5th ISRM Congress. Melbourne, Australia (1983).

[11] Hartman W., Lecinq B., Higgs J., Tongue D. Non destructive integrity testing of rock reinforcement elements in Australian mines. Underground Coal Operators' Conference (2010).

[12] Knape P. Boltometer testing of reference bolt in the final repository for reactor waste (SFR), Forsmark. INIS:SV-UB–1988-15. Sweden (1988).

[13] Starkey A., Ivanovic A., Neilson R. D., Rodger A.A. The integrity testing of ground anchorages using Granit. 20-th International Conference on Ground Control in Mining. USA (2001).

[14] Starkey A., Ivanovic A., Neilson R. D., Rodger A.A. Using a lumped dynamic model of rock bolt to produce training data for neural network for diagnosis of real data. Meccanica 38: 131-142. Kluwer Academic Publishers (2003).

[15] Hao Y., Wu Y., Li P., Tao J., Teng Y., Hao G. Non-destructive inspection on anchorage defect of hollow grouted rock bolt using wavelet transform analysis. Journal on Image and Video Processing 146 (2018).

[16] Patil D.P., Maiti S.K. Experimental verification of a method of detection of multiple cracks in beams based on frequency measurements, **Journal of Sound and Vibration**: 439-451 (2005).

[17] Sadettin O. Analysis of free and forced vibration of a cracked cantilever

beam. **NDT&E International** Vol.40, Issue 6: 443-450 (2007).

[18] Sinha J.K., Friswell M.I. Simulation of the dynamic response of a cracked beam. **Computers & Structures**, Vol. 80, Issues 18-19: 1473-1476 (2002).

[19] Gangbing S., Weijie Li, Bo Wang, Siu Chun M. H. A Review of Rock Bolt Monitoring Using Smart Sensors. Sensors 2017, 17, 776; doi:10.3390/s17040776.

[20] *Hyett, A., Mitri, H., Spearing, A.* Validation of two new technologies for monitoring the in situ performance of rock bolts. Proceedings of the 7th International Symposium on Rockbolting and Rock Mechanics in Mining. AIMS 2012, Aachen: 177-190.

[21] Godfrey DE, Kuchar NR Method of testing the integrity of installed rock bolts. United States Patent US4062229A (1977).

[22] Ewins D.J. Modal Testing: theory, practice and application. Research Studies Press Ltd., England (2000).

[23] Maia N.M.M., Silva J.M.M. Theoretical and Experimental Modal Analysis. Research Studies Press Ltd., England (1997).

[24] Remington P. J., Experimental and theoretical Studies of Vibrating Systems, Encyclopedia of Acoustics, Vol. 2, Ch. 63, pp. 715-734, John Wiley & Sons, New York (1997).

[25] Uhl T. Computer Aided Identification of Mechanical Models. WNT, Poland (1997).

[26] Randall R. B. Mechanical Vibration and Shock Measurements, Bruel & Kjaer handbook: 122-129, Naerum (1982).

[27] Dossing O. Structural Testing, Part II: Modal analysis and Simulation. Bruel & Kjaer, Denmark (1988).

[28] Tryon R.C. Cluster Analysis. Ann Arbor, MI: Edwards Brothers (1939).

[29] Cała M., Flisiak J., Tajduś A. The mechanism of interaction between rockbolt support system and rock strata of inconsistent layers positioning. Polish Academy of Science, Cracow (2001).

[30] Haneol K., Hafeezur R., Wahid A., Abdul Muntaqim N., Jung-Joo K., Jonguk K., Hankyu Y. Classification of Factors Affecting the Performance of Fully Grouted Rock Bolts with Empirical Classification Systems. Applied Sciences, 9, 4781 (2019).